HHS Public Access

Author manuscript

Nature. Author manuscript; available in PMC 2010 October 01.

Published in final edited form as:

Nature. 2010 April 29; 464(7293): 1357–1361. doi:10.1038/nature08938.

NLRP3 inflamasomes are required for atherogenesis and activated by cholesterol crystals that form early in disease

Peter Duewell[1,3,*], **Hajime Kono**[2,*], **Katey J. Rayner**[4,5], **Cherilyn M. Sirois**[1], **Gregory Vladimer**[1], **Franz G. Bauernfeind**[6], **George S. Abela**[9], **Luigi Franchi**[8], **Gabriel Nuñez**[8], **Max Schnurr**[3], **Terje Espevik**[10], **Egil Lien**[1], **Katherine A Fitzgerald**[1], **Kenneth L. Rock**[2], **Kathryn J. Moore**[4,5], **Samuel D Wright**[11], **Veit Hornung**[5,*], and **Eicke Latz**[1,7,10,*]

[1]Department of Infectious Diseases and Immunology, University of Massachusetts Medical School, Worcester, MA

[2]Department of Pathology, University of Massachusetts Medical School, Worcester, MA

[3]Department of Medicine, Division of Gastroenterology, University of Munich, Munich, Germany

[4]Leon H. Charney Division of Cardiology, New York University, New York, NY, USA

[5]Harvard Medical School, Lipid Metabolism Unit, Massachusetts General Hospital, Boston, MA, USA

[6]Institute of Clinical Chemistry und Pharmacology, University Hospitals, University of Bonn, Bonn, Germany

[7]Institute of Innate Immunology, University Hospitals, University of Bonn, Bonn, Germany

[8]Department of Medicine, Division of Cardiology, Michigan State University, East Lansing, MI, USA

[9]Department of Pathology, University of Michigan Medical School, Ann Arbor, MI

[10]Institute of Cancer Research and Molecular Medicine, Norwegian University of Science and Technology, Trondheim, Norway

[11]Cardiovascular Therapeutics, CSL Limited, Melbourne, Australia

The inflammatory nature of atherosclerosis is well established but the agent(s) that incite inflammation in the artery wall remain largely unknown. Germ-free animals are susceptible to atherosclerosis, suggesting that endogenous substances initiate the inflammation1. Mature atherosclerotic lesions contain macroscopic deposits of cholesterol crystals in the necrotic

Corresponding authors: Eicke Latz, MD PhD, Division of Infectious Diseases and Immunology, University of Massachusetts Medical, School, 364 Plantation St, LRB 308, Worcester, MA 01605, USA, Phone: +1 508 856 5889; Fax: +1 508 856 5463; eicke.latz@umassmed.edu and Institute of Innate Immunity, University Hospitals, University of Bonn, Sigmund-Freud-Str. 25, 53127 Bonn, Germany, Phone: +49 228 287 51223; Fax: +49 228 287 51221; eicke.latz@uni-bonn.de, Veit Hornung, MD, Institute of Clinical Chemistry and Pharmacology, University Hospitals, University of Bonn, Sigmund-Freud-Str. 25, 53127 Bonn, Germany, Phone: +49 228 287 12170; veit.hornung@uni-bonn.de.

*These authors contributed equally to this work

Supplementary Information

Supplementary information accompanies this paper.

core but their appearance late in atherogenesis had been thought to disqualify them as primary inflammatory stimuli. However, using a novel microscopic technique, we revealed that minute cholesterol crystals are present in early diet-induced atherosclerotic lesions and that their appearance coincides with the first appearance of inflammatory cells.

Other crystalline substances can induce inflammation by stimulating the caspase-1-activating NLRP3 inflammasome2,3, which results in cleavage and secretion of IL-1 family cytokines. Here, we demonstrate that cholesterol crystals also activate the NLRP3 inflammasome in phagocytes *in vitro* in a process that involves phago-lysosomal damage. Similarly, when injected intraperitoneally, cholesterol crystals induce acute inflammation, which is impaired in mice deficient in components of the NLRP3 inflammasome, cathepsin B, cathepsin L, or IL-1 molecules. Moreover, when low-density lipoprotein receptor (LDLR) deficient mice were reconstituted with NLRP3-, ASC-, or IL-1α/β-deficient bone marrow and fed a high cholesterol diet, they had markedly reduced early atherosclerosis and inflammasome-dependent IL-18 levels.

Our results demonstrate that crystalline cholesterol acts as an endogenous danger signal and its deposition in arteries or elsewhere is an early cause rather than a late consequence of inflammation. These findings provide new insights into the pathogenesis of atherosclerosis and point to new potential molecular targets for the therapy of this disease.

Cholesterol, an indispensable lipid in vertebrates, is effectively insoluble in aqueous environments and elaborate molecular mechanisms have evolved that regulate cholesterol synthesis and its transport in fluids4. Cholesterol crystals are recognized as a hallmark of atherosclerotic lesions5 and their appearance helps in the histopathological classification of advanced atherosclerotic lesions6. However, crystalline cholesterol is soluble in the organic solvents used in histology, so that the presence of large crystals is identifiable but only indirectly as so-called cholesterol crystal clefts, which delineate the space that was occupied before sample preparation. The large cholesterol crystal clefts in atherosclerotic plaques were typically only observed in advanced lesions and, therefore, crystal deposition was thought to arise late in this disease. However, given that atherosclerosis is intimately linked to cholesterol levels, we were interested to determine when and where cholesterol crystals first appear during atherogenesis.

We fed atherosclerosis-prone Apo-E-deficient mice a high cholesterol diet to induce atherosclerosis7,8 and used a combination of laser reflection and fluorescence confocal microscopy3 to identify crystalline materials and immune cells. Many small crystals appeared as early as two weeks after the start of atherogenic diet within small accumulations of subendothelial immune cells in very early atherosclerotic sinus lesions (Fig. 1a, b and Supplementary Fig. 1, 2). The reflective material was identified as being mostly cholesterol crystals by fillipin staining (not shown). Crystal deposition and immune cell recruitment increased steadily with diet feeding and the appearance of crystals correlated with that of macrophages (r_2=0.99, $p<0.001$) (Fig. 1a-d). Cholesterol crystals were not only detected in necrotic cores but also in subendothelial areas that were rich in immune cells. Confocal imaging revealed crystals to localize both inside and outside of cells (Fig. 1b), whereas in corresponding H&E stained sections that were treated with organic solvents during the

staining process cholesterol crystal clefts were visible only after 8 weeks of diet and smaller crystals remained invisible (Fig. 1a). As expected, we failed to detect macrophages or accumulation of crystals in the aortic sinus sections in mice on a regular chow diet (Fig. 1a, b; bottom panel). Additional observations in human advanced atherosclerotic lesions showed that areas rich in immune cells also contained smaller crystals inside and outside of cells in addition to the larger crystals that would leave cholesterol crystal clefts in standard histology (Supplementary Fig. 3, 4). These studies establish that crystals emerge at the earliest time points of diet-induced atherogenesis together with the appearance of immune cells in the subendothelial space.

Various crystals that are linked to tissue inflammation, as well as pore-forming toxins or extracellular ATP, can activate IL-1 family cytokines via triggering of NLRP39. Of note, NLRP3 inflammasome formation requires a priming step that can be provided by pattern recognition or cytokine receptors that activate NF-κB. Cellular priming leads to induction of pro-forms of IL-1 family cytokines and NLRP3 itself, a step, which is required for NRLP3 activation at least *in vitro*10. To test whether cholesterol crystals could activate the release of IL-1β, we incubated LPS-primed human PBMCs with cholesterol crystals. Cholesterol crystals induced a robust, dose-responsive release of cleaved IL-1β in a caspase-1 dependent manner (Fig. 2a, b). Of note, cholesterol crystals added to unprimed cells did not release IL-1β into the supernatant indicating the absence of any contaminants that would be sufficient for priming of cells (Fig. 2a)10. IL-1 cytokines are processed by caspase-1, which can be activated by various inflammasomes9. Since the NLRP3 inflammasome has been reported to recognize a variety of crystals, we next stimulated macrophages from mice deficient in NLRP3 inflammasome components. Cholesterol crystals induced caspase-1 cleavage and IL-1β release in wild-type but not NLRP3- or ASC-deficient macrophages (Fig. 2c, d). Transfected dsDNA (dAdT), a control activator that induces the AIM-2 inflammasome11, activated caspase-1 and induced IL-1β release in an ASC-dependent yet NLRP3-independent manner, as expected (Fig. 2c, d). In addition, mouse macrophages also produced cleaved IL-18, another IL-1 family member that is processed by inflammasomes (Fig. 2e). We also found that chemically pure synthetic cholesterol crystals activated the NLRP3 inflammasome providing further evidence that cholesterol crystals themselves rather than contaminating molecules were the biologically active material (Supplementary Fig. 5a). Notably, priming of cells for NLRP3 activation could be achieved by other pro-inflammatory substances such as cell wall components of Gram-positive bacteria (Supplementary Fig. 5b). Moreover, minimally modified LDL also primes cells for NLRP3 activation (Supplementary Fig. 5c)12. Together, these data establish that crystalline cholesterol leads to NLRP3 inflammasome activation in human and mouse immune cells.

Several hypotheses regarding the molecular mechanisms of NLRP3 inflammasome activation have been formulated3,13. To further elucidate the mechanisms involved in cholesterol crystal recognition, we pharmacologically inhibited phagocytosis with cytochalasin D or lantriculin A and found that these agents inhibited NLRP3 inflammasome activation by crystals (Fig. 3 and Supplementary Fig. 6 a, c, d). In contrast, these inhibitors did not block the activation of the NLRP3 inflammasome by the pore-forming toxin nigericin or the AIM2 activator dAdT (Fig. 3a and Supplementary Fig. 6a, c, d). To follow

the fate of the internalized particles, we performed combined confocal reflection and fluorescence microscopy in macrophages incubated with cholesterol crystals. This analysis revealed that cholesterol crystals induced profound swelling in a fraction of cells (Fig. 3b) as observed for other aggregated materials3,14. Phago-lysosomal membranes contain lipid raft components15, which allowed us to stain the surface of cells with the raft marker choleratoxin B labeled with one fluorescent color and additionally label internal phago-lysosomal membranes after cell permeabilization with differently fluorescing choleratoxin B. Indeed, in macrophages that had previously ingested cholesterol crystals this staining revealed that some cholesterol crystals lacked phago-lysosomal membranes and resided in the cytosol of a fraction of cells, thus indirectly indicating crystal-induced phago-lysosomal membrane rupture (Fig. 3c). This finding was further supported by crystal-induced translocation of soluble lysosomal markers into the cytosol (see below). Additionally, in mouse macrophages cholesterol crystals dose-responsively led to a loss of lysosomal acridine orange fluorescence further confirming lysosomal disruption (Fig. 3d). These studies suggest that cholesterol crystals induced lysosomal damage in macrophages leads to the translocation of phago-lysosomal content into the cytosol. In further experiments we found that the inhibition of lysosomal acidification or cathepsin activity blocked the ability of cholesterol crystals to induce IL-1β secretion (Fig. 3e). Likewise, analysis of cells from mice deficient in single cathepsins (B or L) also showed that cholesterol crystals led to a diminished IL-1β release when compared to wild-type cells. However, the dependency of cholesterol crystal-induced IL-1β release on single cathepsins was less pronounced at higher doses suggesting functional redundancy of cathepsin B and L or potentially additional proteases (Fig. 3f). Together, these experiments suggest that cholesterol crystals induce translocation of lysosomal proteolytic contents, which can be sensed by the NLRP3 inflammasome by as yet undefined mechanisms.

It has previously been demonstrated that oxidized LDL, a major lipid species deposited in vessels, has the potential to damage lysosomal membranes16. We found that macrophages incubated with oxidized LDL internalized this material and nucleated crystals in large, swollen, phago-lysosomal compartments (Fig. 3g); and in some cells these compartments ruptured with translocation of the fluorescent marker dye into the cytosol (Fig. 3g, arrows). A time course analysis revealed that small crystals appeared as early as one hour after incubation with oxidized LDL (not shown) and larger crystals were visible after longer incubation times (Fig. 3h). It is likely that cholesterol crystals form due to the activity of acid cholesterol ester hydolases, which transform cholesteryl esters supplied by oxidized LDL into free cholesterol. As indicated above, minimally modified LDL can prime cells for the NLRP3 inflammasome activation (Supplementary Fig. 5c). Recent evidence suggests that this priming proceeds via the activation of a TLR4/6 homodimer and CD3612. This, together with the propensity of minimally modified LDL to form crystals and to rupture lysosomal membranes, suggests that these LDL species could be sufficient to provide both signals 1 and 2 needed to activate IL-1β release from cells. Indeed, after 24 h incubation we observed spontaneous release of IL-1β in the absence of further NLRP3 inflammasome stimulation (Fig. 3i).

In murine atherosclerotic lesions we identified not only macrophages and dendritic cells but also neutrophils accumulated within the intima space (see Supplementary Fig. 2). IL-1β

plays a key role in the recruitment of neutrophils, and the IL-1-dependent intraperitoneal accumulation of neutrophils has frequently been used as an *in vivo* assay for inflammasome activation and IL-1 production2,17,18. Using this acute inflammation model we found that cholesterol crystals induced a robust induction of neutrophil influx into the peritoneum (Fig. 4a). Neutrophil influx into the peritoneum after cholesterol crystal deposition was markedly reduced in mice lacking IL-1 or the IL-1 receptor (IL-1R), indicating that IL-1 production is indeed induced and essential for cholesterol crystal-induced inflammation *in vivo*. Moreover, mice lacking NLRP3 inflammasome components or cathepsins B or L also recruited significantly fewer neutrophils into the peritoneum after cholesterol crystal injection than wild-type mice. However, the reduction in neutrophilic influx observed after cholesterol crystal deposition was more pronounced in mice lacking IL-1 related genes than in mice lacking NLRP3 inflammasome related genes (Fig. 4a), presumably because of the contribution of IL-1α signaling and/or caspase-1-independent processing of IL-1β19 *in vivo*. In any case, these data confirm that cholesterol crystals trigger NLRP3 inflammasome-dependent IL-1 production *in vivo*.

To test whether the NLRP3 inflammasome is involved in the chronic inflammation that underlies atherogenesis in vessel walls, we tested whether the absence of NLRP3, ASC or IL-1 cytokines might modulate atherosclerosis development in LDLR-deficient mice20, a model for familial hypercholesterolemia. We reconstituted lethally irradiated LDLR-deficient mice with bone marrow from wild-type or NLRP3-,ASC- or IL1α/β-deficient mice and subjected these mice to 8 weeks of a high cholesterol diet. In these radiation bone marrow chimeras, the LDLR-deficiency radioresistant parenchyma causes the animals to become hypercholesterolemic when placed on a high fat diet, while their bone-marrow derived macrophages and other leukocytes lack the NLRP3-inflammasome or IL-1 pathway components needed to respond to cholesterol crystals. We found that the different groups of mice had similar levels of elevated blood cholesterol (not shown). However, mice reconstituted with NLRP3-, ASC-, or IL-1α/b-deficient bone marrow showed significantly lower plasma IL-18 levels, an IL-1 family cytokine whose secretion is dependent on inflammasomes and a biomarker known to be elevated in atherosclerosis21 (Fig. 4b). Additionally, and most importantly, mice whose bone marrow-derived cells lacked NLRP3 inflammasome components or IL-1 cytokines were markedly resistant to developing atherosclerosis (Fig. 4c, d). The lesional area in the aortas of these mice was reduced on average by 69% compared to chimeric LDLR-deficient mice that had wild-type bone marrow. These data demonstrate that activation of the NLRP3 inflammasome by bone marrow derived cells is a major contributor to diet-induced atherosclerosis in mice.

The molecules that incite inflammation in atherosclerotic lesions have presented a long-standing puzzle. While the lesions are absolutely dependent on cholesterol, this abundant, naturally occurring molecule has been viewed as inert. Here, we show that the crystalline form of cholesterol can induce inflammation. The magnitude of the inflammatory response and the mechanism of NRLP3 activation appear identical to that of crystalline uric acid, silica and asbestos2,3,13. All these crystals are known to provoke clinically important inflammation as seen in gout, silicosis and asbestosis, respectively.

The chronic inflammation in gout, silicosis and asbestosis is thought to derive from the inability of cells to destroy the ingested aggregates leading to successive rounds of apoptosis and reingestion of the crystalline material22. In the same way, immune cells cannot degrade cholesterol and depend, instead, on exporting the cholesterol to HDL particles, which carry the cholesterol to the liver for disposal. The success of this or any cellular mechanism in clearing crystals may thus depend on the availability of HDL. Low blood HDL levels are among the most prominent risk factors for atherosclerotic disease23, and pharmacologic means for increasing HDL are being actively pursued as treatments.

Even though cholesterol cannot be degraded by peripheral cells it may be transformed to cholesteryl ester by the cellular enzyme, acylcoenzyme A:cholesterol acyltransferase (ACAT). Cholesteryl esters form droplets rather than crystals and are considered a storage form of cholesterol4. On the assumption that reduced cholesterol storage would be beneficial for reducing atherosclerosis, ACAT inhibitors were tested in large clinical trials. Studies with two such inhibitors showed not a decrease but an increase in the size of the coronary atheroma24,25. This apparent paradox may be reconciled by our findings that the crystalline form of cholesterol, which would be expected to be increased after inhibition of ACAT, may be key in driving arterial inflammation. Indeed, murine studies of ACAT-deficiency show enhanced atherogenesis with abundant cholesterol crystals26. Based on our findings, therapeutic strategies that would reduce cholesterol crystals or block the inflammasome pathway would be predicted to have clinical benefit by reducing the initiation or progression of atherosclerosis. In this context our findings also point to novel molecular targets for the development of therapeutics to treat this disease.

Methods summary

Mice

Mice were kindly provided as follows: NLRP3$^{-/-}$ and ASC$^{-/-}$ (Millenium Pharmaceuticals); Caspase-1$^{-/-}$ (R. Flavell, Yale University, New Haven, CT). Cathepsin B$^{-/-}$ (T. Reinheckel, Albert-Ludwigs-University, Freiburg, Germany), Cathepsin L$^{-/-}$ (H. Ploegh, Whitehead Institute, Cambridge, MA), IL-1$\alpha^{-/-}$ IL-1$\beta^{-/-}$, IL-1$\alpha^{-/-}\beta^{-/-}$ (Yoichiro Iwakura, The Institute of Medical Sciences, The University of Tokyo, Tokyo, Japan). B6-129 (mixed background), C57BL/6, IL-1R$^{-/-}$, ApoE$^{-/-}$ and LDLR$^{-/-}$ mice were purchased from The Jackson Laboratories. Animal experiments were approved by the UMass and Massachusetts General Hospital Animal Care and Use Committees.

Cell culture media and reagents

Immortalized macrophage cell lines and bone-marrow derived cells were cultured as described3 and primed with 10 ng/ml LPS for 2h prior to addition of inflammasome stimuli. Inhibitors were added 30 min prior to stimuli. Crystals and dAdT were applied 6h, ATP (5 mM) and nigericin (10 μM) 1h before supernatant was collected. Poly(dA:dT) was transfected using Lipofectamine 2000 (Invitrogen). Human PBMCs were freshly isolated by Ficoll-Hypaque gradient centrifugation, grown in RPMI medium (Invitrogen), 10% FBS (Atlas Biologicals) 10μg/ml ciprofloxacin (Celgro) at 2×10^5 cells per 96 well and primed

with 50 pg/ml LPS for 2 hours before addition of inflammasome stimuli. Supernatants were assessed for IL-1β by ELISA and western blot.

Neutrophil recruitment to peritoneal cavity

Mice were intraperitoneally injected with 2 mg of cholesterol crystals in 200 μl PBS or PBS alone. After 15 hours, peritoneal lavage cells were stained with fluorescently conjugated mAbs against Ly-6G (Becton Dickinson, clone 1A8) and 7/4 (Serotec) in the presence of mAb 2.4G2 (FcgRIIB/III receptor blocker). The absolute number of neutrophil (Ly-6G+ 7/4+) was determined by flow cytometry.

Methods

Reagents

Bafilomycin A1, cytochalasin D and zYVAD-fmk were from Calbiochem. ATP, acridine orange and poly(dA:dT) sodium salt were form Sigma-Aldrich and ultra-pure LPS was purchased from Invivogen. Nigericin, Hoechst dye, DQ ovalbumin and fluorescent choleratoxin B were purchased from Invitrogen. MSU crystals were prepared as described17.

Cholesterol crystal preparation

Tissue-culture grade or synthetic cholesterol was purchased from Sigma, solubilized in hot acetone and crystallized by cooling. After 6 cycles of recrystallizations, the final crystallization was performed in the presence of 10% endotoxin-free water to obtain hydrated cholesterol crystals. Cholesterol crystals were analyzed for purity by electron impact GC/MS and thin layer chromatography using silica gel and hexane-ethyl acetate (80:20) solvent. Crystal size was varied using a microtube tissue grinder. Fluorescent cholesterol was prepared by addition of the DiD or DiI dyes (Invitrogen) in PBS.

ELISA and Western Blot

ELISA measurements of IL-1β (Becton Dickinson) and IL-18 (MBL International) were made according to the manufacturer's directions. Experiments for caspase-1 Western blot analysis were performed in serum-free DMEM medium. After stimulations, cells were lysed by the addition of a 10X lysis buffer (10% NP-40 in TBS and protease inhibitors), and post-nuclear lysates were separated on 4–20% reducing SDS-PAGE. Anti murine caspase-1 pAb was kindly provided by P. Vandenabeele (University of Ghent, The Netherlands). Anti-human cleaved IL-1β (Cell Signaling) from human PBMCs was analyzed in serum-free supernatants as above without cell lysis.

Confocal microscopy

$ApoE^{-/-}$ mice that were maintained in a pathogen-free facility were fed a Western-type diet (Teklad Adjusted Calories 88137; 21% fat (wt/wt), 0.15% cholesterol (wt/wt) and 19.5% casein (wt/wt); no sodium cholate) starting at 8 weeks of age and continued for 2, 4, 8 or 12 weeks (three mice in each group). Mice were euthanized and hearts were collected as described27. Hearts were serially sectioned at the origins of the aortic valve leaflets, and

every third section (5 μm) was stained with hematoxylin and eosin and imaged by light microscopy. Adjacent sections were fixed in 4% paraformaldehyde, blocked and permeabilized (10% goat serum / 0.5% saponin in PBS) and stained with fluorescent primary antibodies against macrophages (MoMa-2, Serotec), DCs (CD11c, Becton Dickinson) or neutrophils (anti-Neutrophil, Serotec) for 1 h at 37 °C for imaging by confocal microscopy.

Human atherosclerotic lesions were obtained directly after autopsy, serially sectioned at 2- to 3-mm intervals and frozen sections (5 mm) were prepared as above. Parallel sections were stained with Masson's trichrome stain. Tissues were prepared for microscopy as above. Macrophages were stained with anti-CD68 (Serotec), smooth muscle cells were visualized with fluorescent phalloidin (Invitrogen). Human and mouse samples were counterstained with Hoechst dye to visualize nuclei. The atherosclerotic lesions were imaged on a Leica SP2 AOBS confocal microscope where immunofluoroscence staining was visualized by standard confocal techniques and crystals were visualized utilizing laser reflection using enhanced transmittance of the acousto-optical beam splitter as described3. Of note, laser reflection and fluorescence emission occurs at the same confocal plane in this setup. The mean lesion area, amount of crystal deposition and monocyte marker presence was quantified from three digitally captured sections per mouse (Photoshop CS4 Extended). For the quantification of crystal mass and macrophages present, the sum of positive pixels (laser reflection or fluorescence, respectively) was determined and the area calculated from the pixel size. Confocal microscopy of mouse macrophages was performed as described3. DQ ovalbumin only fluoresces upon proteolytic processing and marks phagolysosomal compartments in macrophages.

Acridine orange lysosomal damage assay

This assay was performed by flow cytometry as described3.

Bone marrow transplantation and atherosclerosis model

Eight weeks-old female LDLR$^{-/-}$ mice were lethally irradiated (11 Gy). Bone marrow was prepared from femurs and tibias of C57BL/6, NLRP3$^{-/-}$, ASC$^{-/-}$ and IL-1α$^{-/-}$b$^{-/-}$ donor mice and T cells were depleted using complement (Pel-Freez Biologicals) and anti-Thy1 mAB (M5/49.4.1, ATCC). Irradiated recipient mice were reconstituted with 3.5×10^6 bone marrow cells administered into the tail vein. After 4 weeks, mice were fed with a Western-type diet (Teklad Adjusted Calories 88137; 21% fat [wt/wt], 0.15% cholesterol [wt/wt] and 19.5% casein [wt/wt]; no sodium cholate) for 8 weeks. Mice were euthanized and intracardially perfused with formalin. Hearts were embedded in OTC (Richard-Allen Scientific, Kalamazoo, MI) medium, frozen, and serially sectioned through the aorta from the origins of the aortic valve leaflets and every single section (10 μm) throughout the aortic sinus (800 μm) was collected. Quantification of average lesion area was done from 12 stained with hematoxylin eosin or Giemsa per mouse by two independent investigators with virtually identical results. Serum cholesterol levels were determined by enzymatic assay (Wako Diagnostics), and serum IL-18 was measured by SearchLight protein array technology (Aushon Biosystems, Billerica, MA).

Statistical analyses

The significance of differences between groups was evaluated by one–way analysis of variance (ANOVA) with Dunnett's post- comparison test for multiple groups to control group, or by Student's *t* test for 2 groups. R squared was calculated from the Pearson correlation coefficient. Analyses were done using Prism (GraphPad Software, Inc.).

Supplementary Material

Refer to Web version on PubMed Central for supplementary material.

Acknowledgements

This work was supported by grants of the National Institute of Health (to E.L. and K.L.R) and by the Deutsche Forschungsgemeinschaft (GK 1202, to M.S. and P.D.)

References

1. Wright SD, et al. Infectious agents are not necessary for murine atherogenesis. J Exp Med. 2000; 191:1437–1442. [PubMed: 10770809]
2. Martinon F, Petrilli V, Mayor A, Tardivel A, Tschopp J. Gout-associated uric acid crystals activate the NALP3 inflammasome. Nature. 2006; 440:237–241. [PubMed: 16407889]
3. Hornung V, et al. Silica crystals and aluminum salts activate the NALP3 inflammasome through phagosomal destabilization. Nat Immunol. 2008; 9:847–856. [PubMed: 18604214]
4. Chang TY, Chang CC, Ohgami N, Yamauchi Y. Cholesterol sensing, trafficking, and esterification. Annual review of cell and developmental biology. 2006; 22:129–157.
5. Small DM. George Lyman Duff memorial lecture. Progression and regression of atherosclerotic lesions. Insights from lipid physical biochemistry. Arteriosclerosis. 1988; 8:103–129. [PubMed: 3348756]
6. Stary H, et al. A definition of advanced types of atherosclerotic lesions and a histological classification of atherosclerosis. A report from the Committee on Vascular Lesions of the Council on Arteriosclerosis, American Heart Association. Arterioscler Thromb Vasc Biol. 1995; 15:1512–1531. [PubMed: 7670967]
7. Piedrahita JA, Zhang SH, Hagaman JR, Oliver PM, Maeda N. Generation of mice carrying a mutant apolipoprotein E gene inactivated by gene targeting in embryonic stem cells. Proc Natl Acad Sci U S A. 1992; 89:4471–4475. [PubMed: 1584779]
8. Zhang SH, Reddick RL, Piedrahita JA, Maeda N. Spontaneous hypercholesterolemia and arterial lesions in mice lacking apolipoprotein E. Science. 1992; 258:468–471. [PubMed: 1411543]
9. Martinon F, Mayor A, Tschopp J. The inflammasomes: guardians of the body. Annu Rev Immunol. 2009; 27:229–265. [PubMed: 19302040]
10. Bauernfeind FG, et al. Cutting edge: NF-kappaB activating pattern recognition and cytokine receptors license NLRP3 inflammasome activation by regulating NLRP3 expression. J Immunol. 2009; 183:787–791. [PubMed: 19570822]
11. Hornung V, et al. AIM2 recognizes cytosolic dsDNA and forms a caspase-1-activating inflammasome with ASC. Nature. 2009; 458:514–518. [PubMed: 19158675]
12. Stewart CR, et al. CD36 ligands promote sterile inflammation through assembly of a Toll-like receptor 4 and 6 heterodimer. Nat Immunol. 2009 Dec 27. adv. online pub.
13. Dostert C, et al. Innate immune activation through Nalp3 inflammasome sensing of asbestos and silica. Science. 2008; 320:674–677. [PubMed: 18403674]
14. Halle A, et al. The NALP3 inflammasome is involved in the innate immune response to amyloid-beta. Nat Immunol. 2008; 9:857–865. [PubMed: 18604209]
15. Garin J, et al. The phagosome proteome: insight into phagosome functions. J Cell Biol. 2001; 152:165–180. [PubMed: 11149929]

16. Yuan XM, Li W, Olsson AG, Brunk UT. The toxicity to macrophages of oxidized low-density lipoprotein is mediated through lysosomal damage. Atherosclerosis. 1997; 133:153–161. [PubMed: 9298675]
17. Chen CJ, et al. Identification of a key pathway required for the sterile inflammatory response triggered by dying cells. Nat Med. 2007; 13:851–856. [PubMed: 17572686]
18. Guarda G, et al. T cells dampen innate immune responses through inhibition of NLRP1 and NLRP3 inflammasomes. Nature. 2009
19. Dinarello CA. Immunological and inflammatory functions of the interleukin-1 family. Annu Rev Immunol. 2009; 27:519–550. doi:10.1146/annurev.immunol.021908.132612. [PubMed: 19302047]
20. Ishibashi S, Goldstein JL, Brown MS, Herz J, Burns DK. Massive xanthomatosis and atherosclerosis in cholesterol-fed low density lipoprotein receptor-negative mice. J Clin Invest. 1994; 93:1885–1893. doi:10.1172/JCI117179. [PubMed: 8182121]
21. Blankenberg S, et al. Interleukin-18 is a strong predictor of cardiovascular death in stable and unstable angina. Circulation. 2002; 106:24–30. [PubMed: 12093765]
22. Mossman BT, Churg A. Mechanisms in the pathogenesis of asbestosis and silicosis. Am J Respir Crit Care Med. 1998; 157:1666–1680. [PubMed: 9603153]
23. Gordon T, Castelli WP, Hjortland MC, Kannel WB, Dawber TR. High density lipoprotein as a protective factor against coronary heart disease. The Framingham Study. The American journal of medicine. 1977; 62:707–714. [PubMed: 193398]
24. Nissen SE, et al. Effect of ACAT inhibition on the progression of coronary atherosclerosis. N Engl J Med. 2006; 354:1253–1263. [PubMed: 16554527]
25. Meuwese MC, et al. ACAT inhibition and progression of carotid atherosclerosis in patients with familial hypercholesterolemia: the CAPTIVATE randomized trial. Jama. 2009; 301:1131–1139. [PubMed: 19293413]
26. Accad M, et al. Massive xanthomatosis and altered composition of atherosclerotic lesions in hyperlipidemic mice lacking acyl CoA:cholesterol acyltransferase 1. J Clin Invest. 2000; 105:711–719. [PubMed: 10727439]
27. Moore KJ, et al. Loss of receptor-mediated lipid uptake via scavenger receptor A or CD36 pathways does not ameliorate atherosclerosis in hyperlipidemic mice. J Clin Invest. 2005; 115:2192–2201. [PubMed: 16075060]

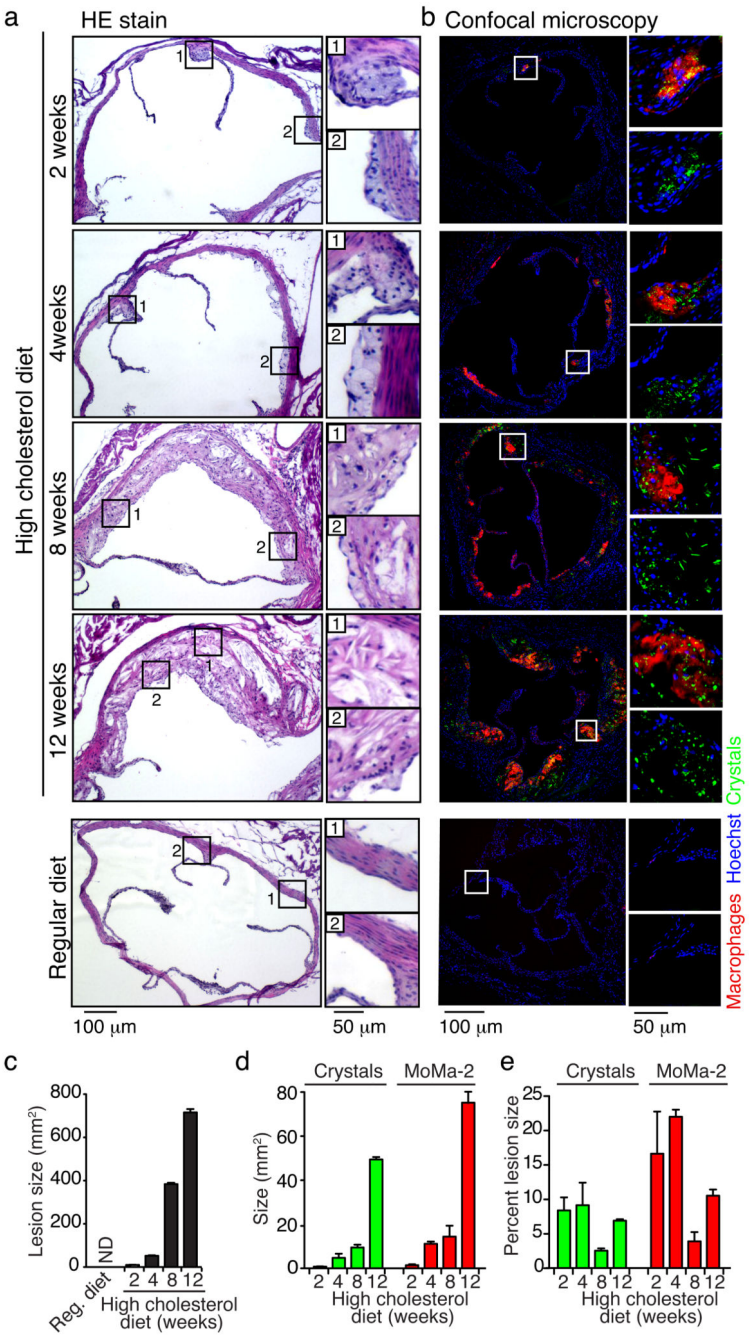

Fig. 1. Cholesterol crystals appear in early atherosclerotic lesions

a, H&E stain and **b**, confocal fluorescence and reflection microscopy of adjacent aortic sinus sections of Apo-E-KO mice fed a high cholesterol diet (upper panels) as indicated or a regular diet (lower panel). Areas in white or black boxes were enlarged; crystal reflection signal is color coded green. **c, d, e,** Quantification of lesion size (c), crystal or macrophage marker MoMa-2 staining amount presented as absolute values (d) or percent of lesions size (e). Representative sections of three mice from each group are shown (a, b). Means and s.e.m. are shown (c, d, e).

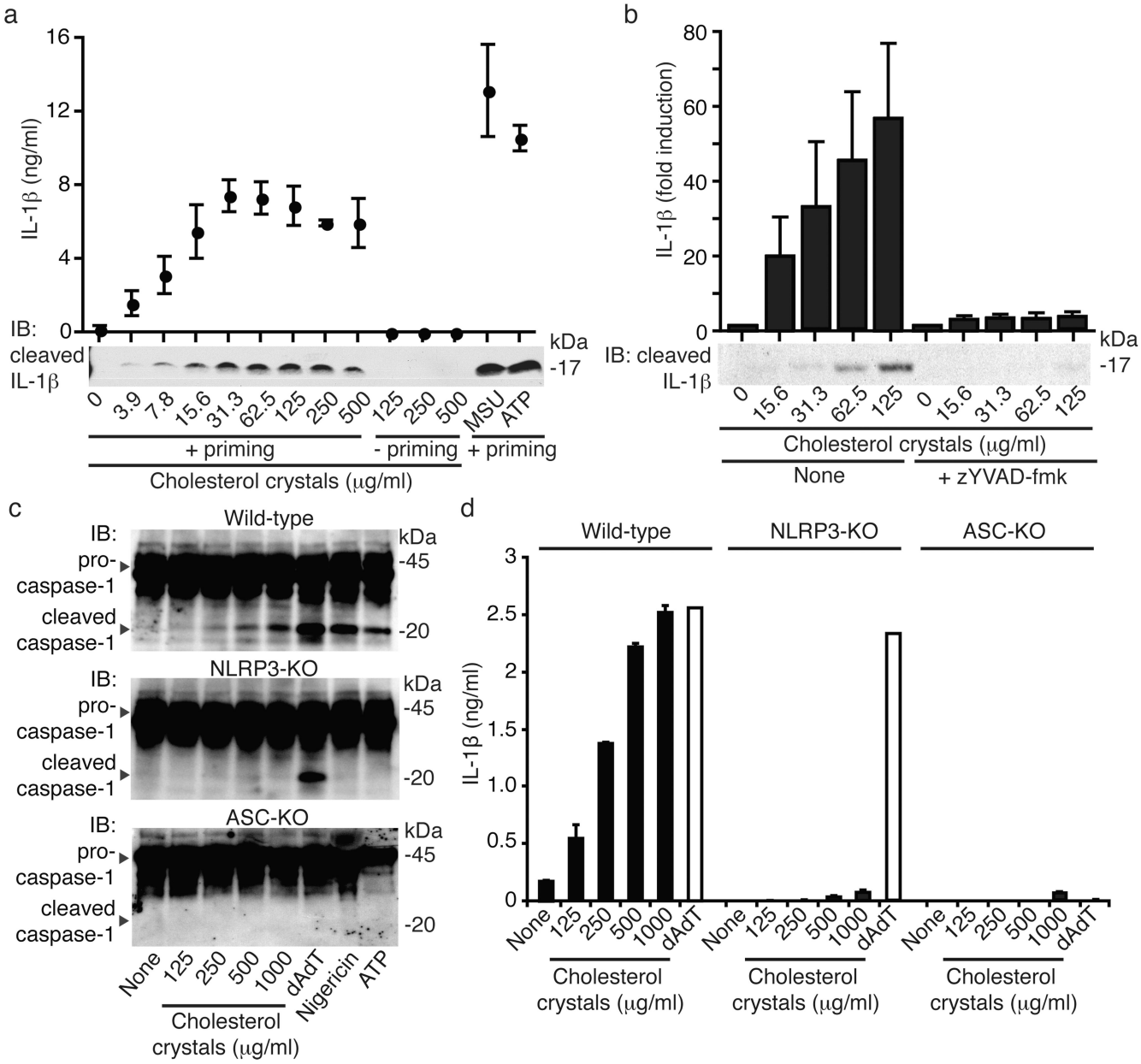

Fig. 2. Cholesterol crystals activate the NLRP3 inflammasome

a, b, Resting or LPS-primed human PBMCs were treated with cholesterol crystals as indicated, MSU crystals (250 μg/ml) or ATP in the presence or absence of the caspase-1 inhibitor zYVAD-fmk (10mM) (b). ELISA and immunoblot (IB) were performed for IL-1β. **c, d,** IB for caspase-1 in supernatants and cell lysates (c) or ELISA for IL-1β in supernatants (d) from LPS-primed wild-type, NLRP3- or ASC-deficient macrophages stimulated with cholesterol crystals, transfected dsDNA (dAdT), nigericin or ATP. **e,** IL-18 ELISA of supernatants from LPS-primed wild-type macrophages stimulated with cholesterol crystals or nigericin. Means and s.e.m. of four donors (a, b) or one out of three independent experiments (c, d, e) are shown.

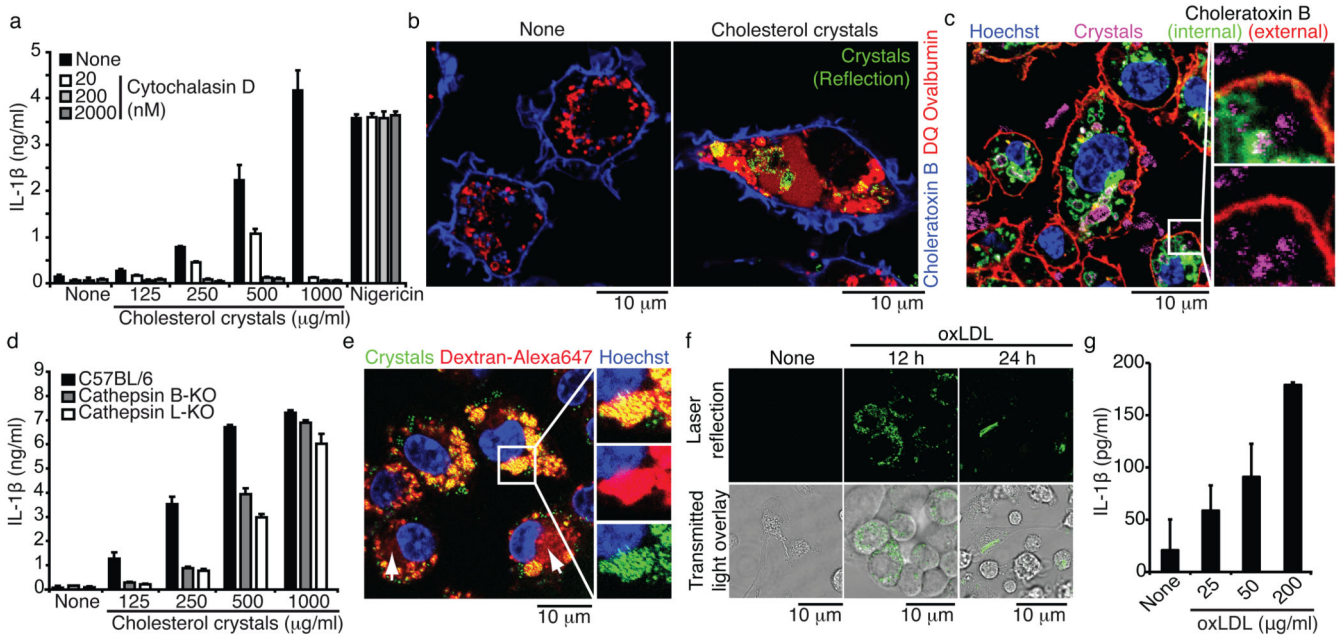

Fig. 3. Cholesterol crystals activate the NLRP3 inflammasome by inducing lysosomal damage

a, IL-1β ELISA of supernatants from LPS-primed murine macrophages stimulated with cholesterol crystals or nigericin in the presence or absence of cytochalasin D. **b, c,** Combined confocal fluorescence and reflection microscopy of murine macrophages incubated with DQ ovalbumin alone (b, left) or together with cholesterol crystals (125 μg/ml) (b, right; c) for 2h and plasma membrane was stained with A647-conjugated choleratoxin B (b, c). **c,** Cells were fixed, permeabilized (0.05% saponin) and internal membranes additionally stained with A555-conjugated choleratoxin B. Nuclei were stained with Hoechst dye. **d,** Murine macrophages stimulated with cholesterol crystals for 6h, stained with acridine orange and analyzed by FACS. **e, f,** IL-1β ELISA of supernatants from LPS-primed, murine macrophages stimulated with cholesterol crystals in the presence or absence of bafilomycin A1 (e) or from LPS-primed wild-type, cathepsin B or L deficient macrophages stimulated with cholesterol crystals (f). **g, h,** Murine macrophages stimulated with 100 μg/ml oxLDL for the indicated times and fluorescent dextran (g, 20h) were imaged by combined confocal fluorescence and reflection microscopy **i,** Unprimed murine macrophages were incubated with oxidized LDL as indicated for 24 h and IL-1β in supernatants was measured by ELISA. (a, d-f, i) One out of three independent experiments are shown; means and s.d. (a, e, f); Representative images of five (b, c) or two (g, h) independent experiments.

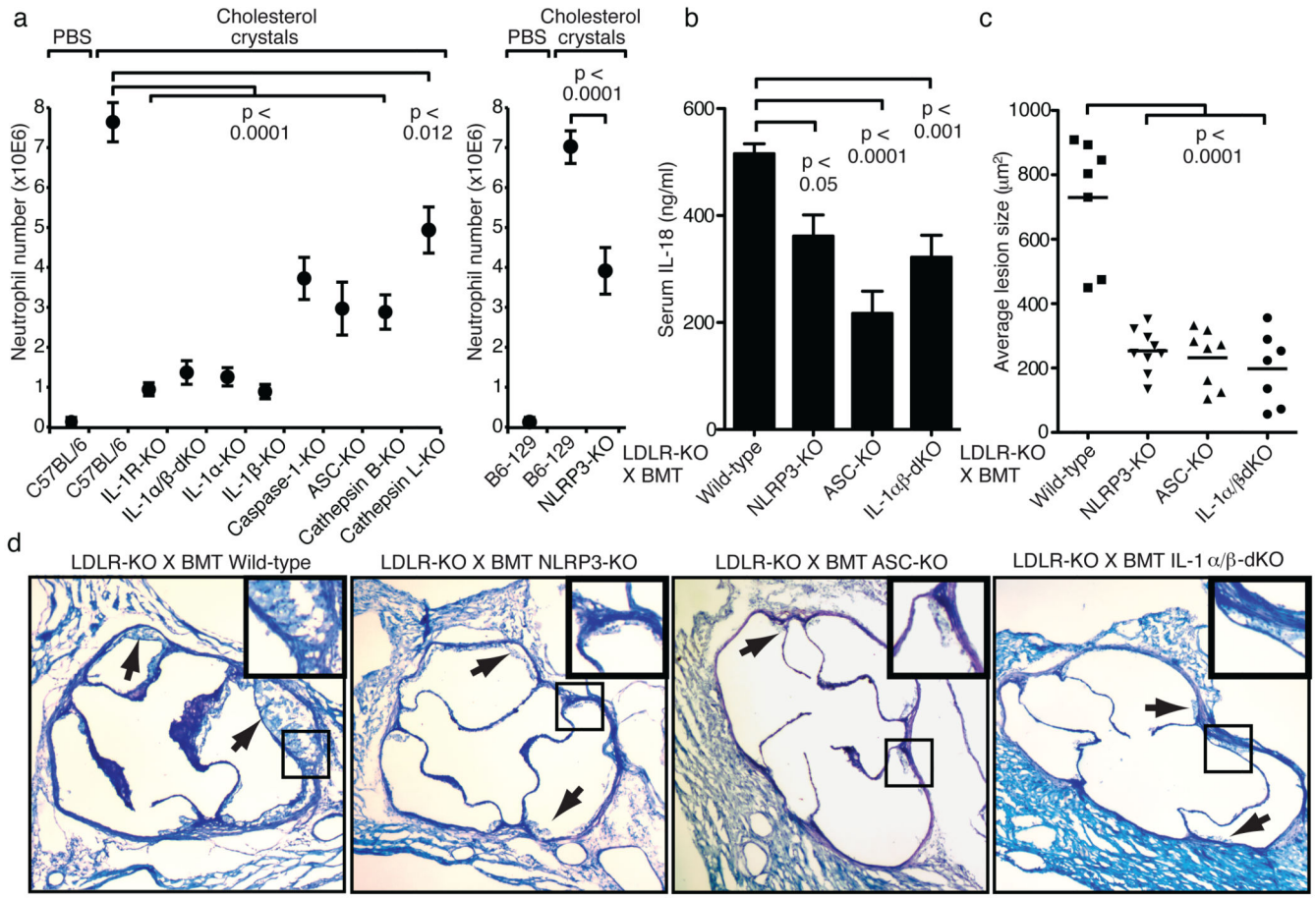

Fig. 4. The NLRP3 inflammasome mediates crystal-induced peritoneal inflammation and atherosclerosis *in vivo*

a, C57BL/6 (n=23), B6-129 (n=13) or mice deficient in genes encoding IL-1R (n=11), IL-1α/b (n=11), IL-1α (n=4), IL-1β (n=4), caspase-1 (n=7), ASC (n=15), cathepsin B (n=10), cathepsin L (n=5), NLRP3 (n=10) were peritoneally injected with cholesterol crystals or PBS (C57BL/6 n=14; B6-129 n=4). Peritoneal lavage cells were analyzed for neutrophils after 15h. Data represent means and s.e.m. from pooled groups of mice out of experiments repeated 2–4 times. **b–d,** Female LDLR-KO mice reconstituted with C57BL/6 (n=7), NLRP3-KO (n=9), ASC-KO (n=8) or IL-1α/b-dKO (n=7) bone marrow were fed a high fat diet for 8 weeks and analyzed for serum IL-18 concentration (b) and average aortic sinus lesion size (c, d). (c) Each dot represents the mean lesion size of serial cross-sections from individual mice. (d) Representative photographs of the aortic sinus stained with Giemsa. Insets show 2-fold magnified portions of the images (black box), arrows point to atherosclerotic lesions.